Kinematic vorticity analysis within the Zagros hinterland involved-basement window, Tutak gneiss dome, southwestern Iran

Akram Alizadeh[1*], Khalil Sarkarinejad[2], Yousef Sattarzadeh[3]

1- Department of Geology, Faculty of Science, Urmia University, Iran. P. O. Box: 57153-165.
2- Department of Earth Sciences, College of Sciences, Shiraz University, Iran. P. O. Box: 71454.
3- Department of Geology, Tabriz University, Iran.

* Corresponding Author: ak.alizadeh@urmia.ac.ir

Received: 15 October2013 / Accepted: 01 December 2013 / Published online: 07 December 2013

Abstract

Dehbid mylonite nappes associated with the Tutak gneiss dome as the Zagros hinterland involved-basement window in the Zagros Orogenic Belt has significant components of dextral sense of shear along the mylonite nappes and are related to the high proportion of simple shear relative to pure shear deformation. Kinematic vorticity analysis (W_k) was made in order to determination of relative amounts of simple shear and pure shear components. The kinematic vorticity analysis has taken as evidence of porphyroclasts rotation relative to internal reference frames during non-coaxial deformation within the Tutak gneiss dome in the Zagros Orogenic Belt. The quartz c-axis preferred orientation evidence used to drive the degree of non-coaxiality during deformation. The mean kinematic vorticity (W_m) value in the Tutak gneiss dome revealed contribution of 48% pure shear and 52% simple shear components. Detailed kinematic vorticity studies may allow this interpretation that the convergence between the Afro-Arabian and central Iran continental crusts is characterized by basement involvement during ongoing inclined dextral transpressional regime.

Keywords: Vorticity, Simple Shear, Gneiss Dome, Zagros, Iran.

1–Introduction

Gneiss domes are important features as the exposed hinterland involved-basement in the orogenic systems (Alizadeh, 2008). More commonly in the last two decades, gneiss domes have been viewed as either contractional or extensional regimes (Whitney *et al*., 2004). For example, genesis of gneiss dome has been ascribed of the crustal shortening; fold interference (Burg *et al*., 1984; Rolland *et al*., 2001); buckling (Hickey and Bell, 2001; Stipska *et al*., 2000), extension which is related to the metamorphic core complex formation (Brun and Van Den Driessche, 1994; Chen *et al*., 1990; Escuder Viruete *et al*., 2000; Yan *et al*., 2003), and extension-assisted diapiric ascent of partially molten lower to middle crust during orogenic collapse (Vanderhaeghe *et al*., 1999).

The ductile shear zones around domes may have experienced dominantly pure-shear deformation (e.g., Lee *et al*., 2000; Vanderhaeghe *et al*., 1999) or simple-shear deformation (e.g., Kündig, 1989). Kinematic vorticity number (W_k) is a measure of the relative amounts of simple shear and pure shear of the flow (Passchier, 1987; Passchier and Trouw, 1996).

The orientation of fixed elements of flow can be found from sets of shortened or stretched of the quartz veins and their quartz c-axis fabrics preferred orientations, and with an assumption of the volume change during deformation. These features can be used to estimate mean kinematic vorticity (W_m). A quantity Wm can also be defined as a parameter of finite deformation and expresses the mean value of Wk. For steady-state deformation $W_k = W_m$ (Passchier, 1987).Rotation of the rigid body relative to the incremental stretching direction during deformation in the regional-scale shear zone is used to determine finite strain pattern and kinematic vorticity number (W_k). Measurements of the kinematic vorticity number from quartz c-axes were used to estimate the simple shear and pure shear components. We also estimated the orientation of principal axes of the strain ellipsoid, the amounts of finite strain and initial shape of undeformed markers.

Mylonites are important separators between tectonic units in orogenic zones (Olesen, 2008). Characteristic features of mylonites are (1) a strong fabric, which reflects the high strain, and (2) a content of porphyroclasts consisting of the rheologically stronger minerals of the precursor, such as feldspar in a quartz matrix (Grunsky *et al*., 1980), quartz in a calcite matrix (Bestmann *et al*., 2000), and orthopyroxene in an olivine matrix (Ishii and Sawaguchi, 2002).

2–Geology and structural setting of the Tutak gneiss dome

The Tutak gneiss dome within the Sanandaj-Sirjan HP-LT metamorphic belt (Sarkarinejad and Azizi, 2008) as the part of the Zagros is involved-basement window of the Zagros Orogenic Belt. This structural window helps to study the deformation phases in the orogenic events related to the convergence between the Afro-Arabian continent and Iranian microcontinent. The field study, structural, microstructural and metamorphic petrology investigations indicate that the Tutak gneiss dome was formed by the contractional and diapiric processes which contributed to the structural evolution and formation of its geometry (Alizadeh *et al*., 2010; Sarkarinejad and Alizadeh, 2009).

The Tutak gneiss dome is cored by two aplite-granite and Bendenow granitic-gneiss that are overlain by schist-zone Silurian and Devonian meta-sedimentary unit and the Kuh-e-Sefid marbles which un-conformably covered by the quartzite-greenschist Surian complex (Fig. 1).

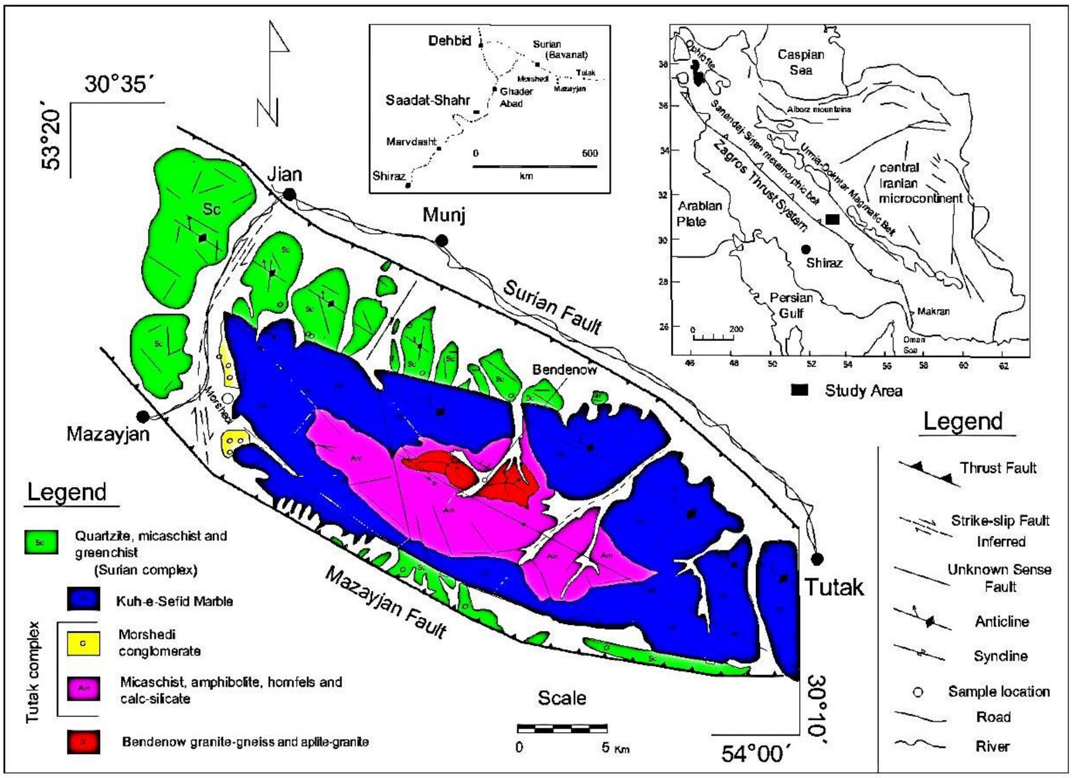

Figure 1) Geological map of the Tutak gneiss dome shows the geographic position and geometric shape of the dome. The thick layers of marble have occupied the Bendenow granite-gneiss and Tutak complex, elliptically. Two mainly schist facies have spaced around thick layer, known as the Surian (outside of the Tutak gneiss dome) and Tutak (inside the dome) complexes.

Two deep-seated mylonite nappes which include the Surian back-thrust nappe at the north and Mazayjan thrust nappe at the south bounded the dome, which exhumed the Tutak gneiss dome (Sarkarinejad and Alizadeh, 2009). These zones joined together in Dehbid region, forming Dehbid ellipse shapped mylonite nappes and are aligned along the Zagros Thrust System with NW-SE trending (Fig. 1). The Tutak gneiss dome is located in the core of an elongated ellipse shaped, doubly plunging anticline with form as the synform which due to the erosion of the relatively incompetent rocks in the core of anticline.

As depicted, there are two undeformed granites plutons within the gneiss domes. These pre- to syn-orogenic plutons generally occur in distinct structural belts of the previously active mobile belt which constitutes the country rocks for these younger intrusions (Sarkarinejad and Alizadeh, 2009).

The two granites plutons of gneiss domes are confined to regions which have been subjected to superposed deformation (Alizadeh *et al*., 2010). In the first stage, an early original aplite-granite was ejected within the core gneiss dome. This granite was later unroofed and was covered by turbiditic younger sediments which containing the basal Morshedi deformed conglomerate. The conglomerate consist pebble of the underlying granite (Alizadeh *et al*., 2010; Sarkarinejad and Alizadeh, 2009). Orogenic forces again were activated since about 180 Ma (Alizadeh *et al*., 2010) and were remobilized the Bendenow granite-gneiss. The sedimentary rocks, generally metamorphosed and deformed at this time, have been intruded by the younger granite. Metamorphic rocks in the area are overlain un-conformably by the Jurassic rocks (Alizadeh, 2008). Particularly where metamorphosed and deformed conglomerate is present, and core/cover contact has been interpreted as a deformed unconformity (Eskola, 1949).

In gneiss dome regions, the contact between the core and metamorphic mantling rocks is commonly represented by a distinctive meta-sedimentary unit such a deformed conglomerate (Vanderhaeghe, 1999). An outcrop of the Morshedi conglomerate lied northwestern part of the Tutak gneiss dome (Alric and Virlogeus, 1977; Fig. 2). The pebbles of Morshedi conglomerate are represented by prolate and oblate in shapes.

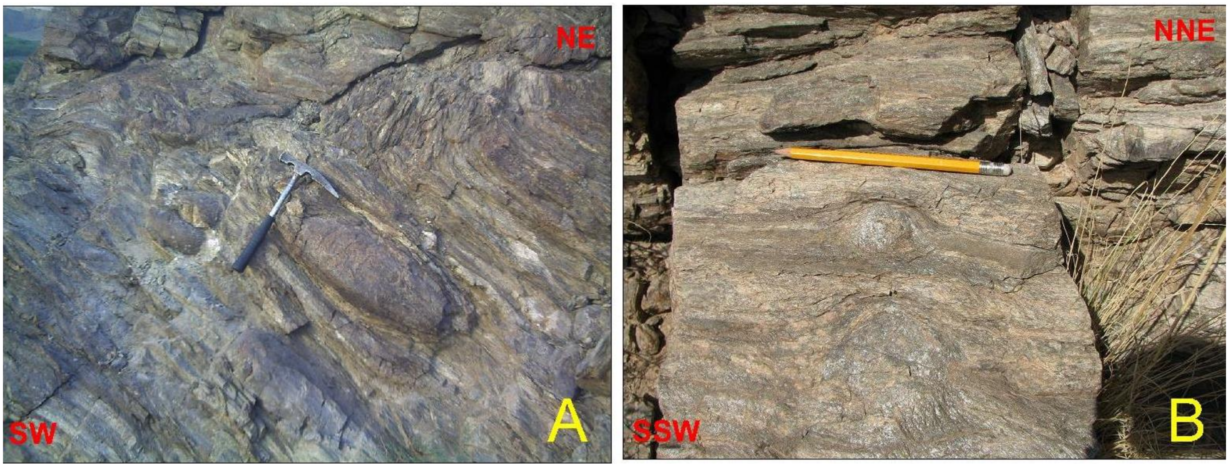

Figure 2) The Morshedi conglomerate. Two shapes of pebble, prolate and oblate, can be distinct at the field. The long axis of prolate pebble aligned at NW-SE trend.

2.1–Finite strain analysis in the Morshedi Basal Conglomerate

The way by which pebbles of conglomerate or other elliptical grains deform is geometrically similar to the results of superimposed deformation; the role of the strain ellipse, after the first deformation, is replaced by the elliptical shape of pebble (Fayon *et al*., 2004; Fig. 3).

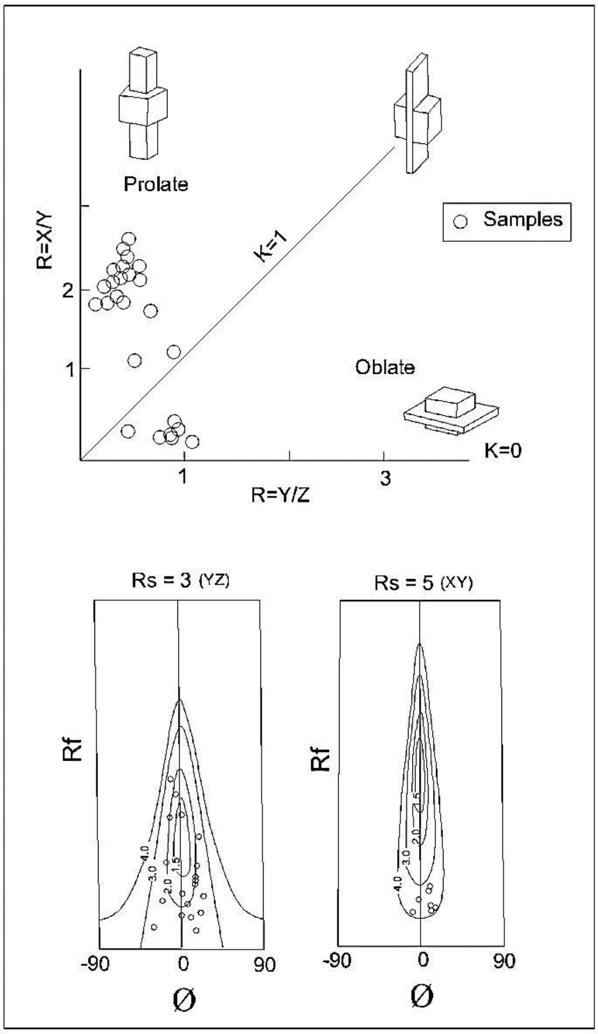

Figure 3) Prolate and oblate shapes of pebbles in Flinn graph. The amount of Rs for prolate shape equals 3, Ri = 2.4, Rs = 5, and Ri for oblate shapes of pebbles is equal 3.6.

The finite strain measurement (planes XY and YZ) on the 93 quartz grains of the flattened and elongated pebbles of the mylonitic microconglomerate (Fig. 4) indicates that the zone is characterized by the Flinn parameter (Flinn, 1979) and ratio of X, Y, and Z axes of the strain ellipsoid equals 2.6:1:0.8. In Rf/Ø Method, the two-dimensional finite strain (Rs) of X/Y and Y/Z planes were plotted verses the angle (ϕ) of Morshedi conglomerate. The results show Rs= 3.9 for XY-plane and 2.8 for YZ-plane respectively. On the graph, also the mean angle of orientation is Ø mean = 28°, and the pebble long axes, have been oriented in the NW-SE and then superposed and trended toward NNE-SSW (Alizadeh, 2008).

2.2–Two dimensional rotation behavior of a rigid ellipse in confined viscous flow

The rotation of rigid elliptical inclusions in simple shear flow for a non-slipping inclusion/matrix interface was studied using a two dimensional finite element numerical model in connection with an adequate computational strategy (Hayward, 1992; Taborda *et al*., 2004). As previously shown by analogue experiments (Marques and Coelho, 2001) the inclusion rotation is strongly affected by the relative confinement.

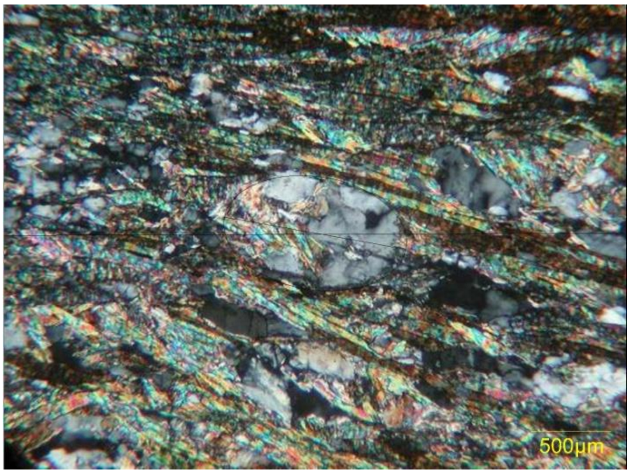

Figure 4) Microphotograph of 2-D rigid body rotation of the grain of Morshedi conglomerate in the Tutak gneiss dome.

The steady-state motion of a viscous, incompressible Newtonian fluid at very low Reynolds number and dynamical Navier–Stokes equations of flow reduce to the Stokes approximation (Taborda *et al*., 2004), were solved on the 2-D rectangular domain illustrated in Figure 4. Kinematic vorticity number was calculated for the Morshedi deformed conglomerate in the Tutak gneiss dome (Fig. 4). The results of computes are given in Table 1. The quartz porphyroclasts have rotated in a clockwise sense relative to the external fabric.

Table 1) Parameters for rigid body rotation at the study area. (Reference lines: H = 120 and L = 204).

e_1	e_2	Φ	H	L	S = H/e_2	ω	R
150	60	30	120	204	20	0.63	1
140	40	32	120	204	30	0.74	1.5

A rigid elliptical body defined by the two principal axes, e1 and e2 (the aspect ratio, R, is equal to e1/e2) was positioned at the center of the domain (X, Y = 0). The width (H) and length (L) of the computational domain were set, respectively, to 2 and 10, so that the flow perturbation due to the presence of the inclusion was observed to be negligible at the boundaries (Fig. 5; [Taborda *et al*., 2004].

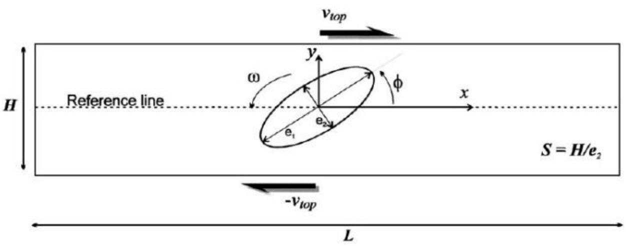

Figure 5) Representation of the computational domain with an elliptical inclusion by Taborda et al. (2004). H and L are the height and length of the domain; e1 and e2 are the principal axes of the elliptical inclusion; Ø is the angle between e1 and shear zone boundaries and W is the inclusion's angular velocity. The shear direction (X) is parallel to the x-axis.

The angle between the instantaneous orientation of the inclusion's longest axis (e1) and the shear direction (X) is Φ, and the inclusion's angular velocity is ω. The initial conditions needed to complete the mathematical formulation and define a simple shear flow were: velocity set to 1 and -1 at the top and bottom boundaries, respectively; velocity set to vary linearly between top and bottom velocities with zero-mean at the left and right end boundaries (Taborda *et al*., 2004). These settings made the shear strain rate ($\dot{\gamma}$) and the vorticity (ω) of the fluid undisturbed by the inclusion to be -1. Therefore, the fluid velocity was assumed equal to the inclusion surface velocity, with a magnitude equal to ω×r, where r (Φ) = | r | is the radial distance to the surface of the inclusion (Taborda *et al*., 2004).

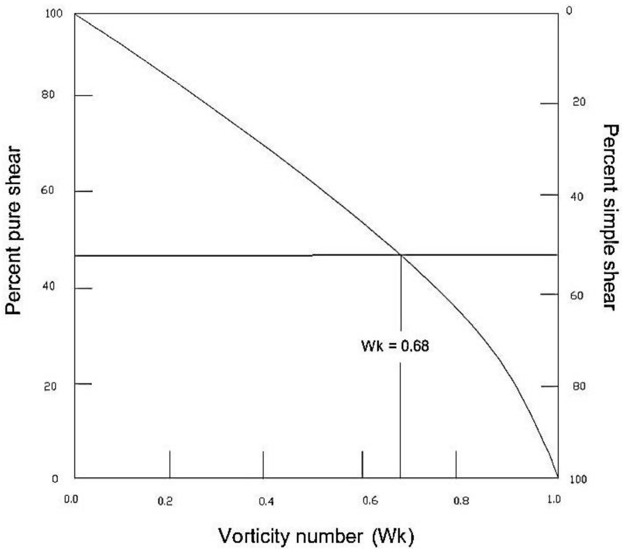

Figure 6) Relation between kinematic vorticity number (W_k) and components of pure and simple shear for instantaneous 2-D flow.

Measurements of the kinematic vorticity number (W_k) the study area indicate that the range of W_k is 0.68. Figure 6 is a graph that represents the percent of pure and simple shear deformation. The mean estimated W_k=0.68 shows that 48% pure shear and 52% simple shear components contributed to ductile flow (Fig. 6).

3–Quartz c-axis patterns

The quartz c-axis fabrics will be reset by dynamic recrystallization so that only the later parts of the deformation history are preserved (Wallis, 1992). There are different phases of deformation in the study area (Alizadeh *et al*., 2010). The later one has been affected the deformed quartz grains.

Oriented samples of quartz were carried out the c-axis of the quartz veins. Optic c-axis measurements were carried out on the thin sections cut perpendicular to the foliation plane (XZ-plane) and parallel to the stretching lineation using a 5-axis U-stage. The c-axis orientation were plotted with respect to the mesoscopic foliation framework on equal area, lower hemisphere stereographic projections and contoured using SpheriStat software to obtain c-axes patterns. The asymmetry in density distribution with respect to the foliation suggests a dextral sense of shear (Sarkarinejad and Alizadeh, 2009). Quartz c-axis studies (Lister and Hobbs, 1980) show that the central girdle of quartz c-axis patterns develops perpendicular to the flow plane in simple shear and pure shear or general shear. Regarding this assumption, the angle between the perpendicular to the central girdle and the foliation is equal to the angle between the flow plane and the flattening plane of strain, β. In the studied samples β is between 10° and 12° and can be plotted on a Mohr circle (Lister and Hobbs, 1980). The angle β is a function of R_{xz} (principal normal strain ratio in the XZ section) and W_k as demonstrated by Wallis (1995):

$$W_k = \sin \{\tan^{-1} [\sin (2\beta) / [(R_{xz}+1) / (R_{xz}-1)] - \cos (2\beta)]\} \times (R_{xz}+1) / (R_{xz}-1)$$

The principal normal strain ratio in the XZ section (R_{xz}) was determined using deformed quartz grains. The estimated quartz c-axis girdle record β angle between 10° – 12°, R_{xz} = 2.6 and $0.6 < W_k < 0.8$; which documented the non-coaxial deformation.

4–Discussion and conclusions

The Tutak gneiss dome within the Dehbid doubly vergent mylonite nappe represents part of the Zagros hinterland involved-basement window along the Zagros thrust system. The basement-involved contains number of asymmetric fabrics which can be used as shear sense indicators and rigid body rotation. Both the rigid body rotation and quartz c-axis patterns developed throughout the period of ductile deformation of the basement. Two techniques of rotated porphyroblast and crystallographic fabric are used to measure kinematic vorticity number. The 2D rigid body rotation of the Morshedi conglomerate pebbles and quartz c-axis fabric were used to estimate the kinematic vorticity number (Fig. 7).

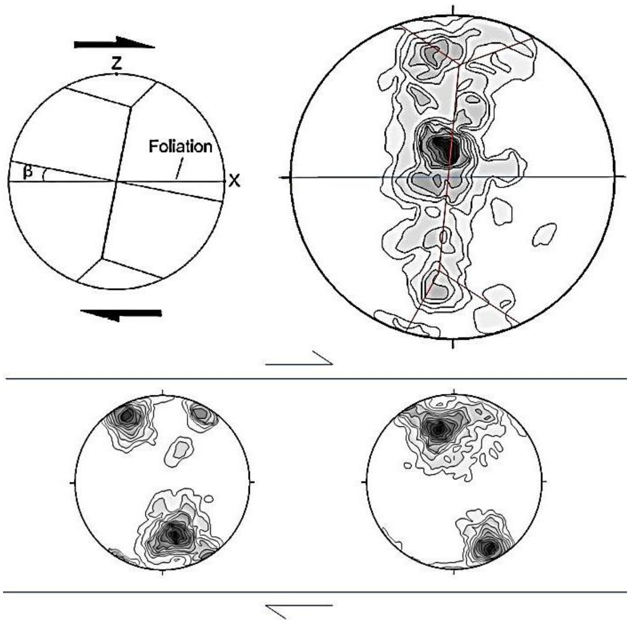

Figure 7) Quartz c-axis fabric measured in the quartz veins of the Tutak gneiss dome. The measurements are displayed on equal-area, lower hemisphere stereographic projection. The foliation is vertical and stretching lineation within the foliation is horizontal. The angle between the normal to the central part of the fabric skeleton and foliation is β, with 10 > β > 12.

The estimated kinematic vorticity number of $W_k = W_m$; 0.68 by the rigid body rotation and $0.6 < W_k < 0.8$ by the quartz c-axis patterns. In steady-state deformation (Law *et al*., 2004) the instantaneous deformation is equal to W_m (finite deformation). The estimated mean finite deformation (W_m) value indicates 48% pure shear component and 52% simple shear component of deformation. The simple shear about 52% with small component of tension is parallel to the lineation.

A deformation path associated $W_m < 1$ causes shortening perpendicular to the flow plane and this could be an important role in the extrusion of the high grade rocks in the study area (Sarkarinejad and Alizadeh, 2009). The ratio of three axes of the strain ellipsoids which obtained from deformed conglomerate pebbles suggesting an apparent contraction type of ductile deformation.

In general, detailed kinematic vorticity studies to determine exact contributions of pure shear and simple shear components in the Tutak gneiss dome which allow the following interpretations:

1) The Dehbid mylonite nappe is part of the NW-SE dextral thrust system related to Zagros Orogenic Belt.

2) Components of simple and pure shear deformation were involved in the formation of the NE-SW contractional regime.

3) Combination of simple shear and pure shear or general shear is results of general non-coaxial flow that characterized by a stretching parallel to the shear zone boundaries, whereas the shortening is oblique; and also, as the Tutak gneiss dome basement window of the continental-scale of transpression between the Afro-Arabian continent and central Iran microcontinent.

4) The convergence of the Afro-Arabian continent and Iranian microcontinent is characterized by dextral deformation and exhumation of the hinterland involved-basement.

Acknowledgments:

The authors would like to thank Dr. B. Samani and an anonymuous reviewer for their kind and careful comments that made the manuscript improved. The support of Urmia University for the first author, and facilities provided by the Earth Science Department of the Shiraz University are gratefully acknowledged.

References:

Alizadeh, A. 2008. Structural evolution of the Tutak gneiss dome.Ph.D dissertation, Shiraz University, 185p.

Alizadeh, A., Lopez Martınez, M., Sarkarinejad K. 2010. ^{40}Ar-^{39}Ar Geochronology in a gneiss dome within the Zagros Orogenic Belt. C. R. Geoscience: 342, 837–846.

Alric, G., Virlogeus, D. 1977. Petrography and Geochemistry study of metamorphic and magmatic in Dehbid-Bavanat Region, Report 21, Geological Survey of Iran .

Bestmann, M., Kunze, K., Matthews, A. 2000. Evolution of a calcite marble shear zone complex on Thassos Island, Greece: microstructural and textural fabrics and their kinematic significance. Journal of Structural Geology: 22, 1789–1807.

Brun, J.-P., Van Den Driessche, J. 1994. Extensional gneiss domes and detachment faults—structure and kinematics. Bulletin de la Société Géologique de France: 165, 519–530.

Burg, J. P., Guiraud, M., Chen, G. M., Li, G. C. 1984. Himalayan metamorphism and deformations in the north Himalayan belt (southern Tibet, China). Earth and Planetary Science Letters: 69, 391–400.

Chen, Z., Liu, Y., Hodges, K. V., Burchfiel, B. C., Royden, L.H., Deng, C. 1990. The Kangmar Dome: A metamorphic core complex in southern Xizang (Tibet). Science: 250, 1552–1556.

Escuder Viruete, J., Indares, A., Arenas, R. 2000. P-T paths derived from garnet growth zoning in an extensional setting: an example from the Tormes Gneiss Dome (Iberian Massif, Spain). Journal of Petrology: 41, 1489–1515.

Eskola, P. E. 1949. The problem of mantled gneiss domes. Geological Society of London, Quarterly Journal: 104, 461–476.

Fayon, A. K., Whitney, D. L., Teyssier, C. 2004. Exhumation of orogenic crust: Diapiric ascent versus low-angle normal faulting. Geological Society of America, Special Paper 380.

Flinn, D. 1979. The deformation matrix and deformation ellipsoid. Journal of Structural Geology: 1, 221–229.

Grunsky, E. C., Robin, P.-Y. F., Schwerdtner, W. M. 1980. Orientation of feldspar porphyroclasts in mylonite samples from the southern Churchill Province, Canadian Shield. Tectonophysics: 66, 213–224.

Hayward, N. 1992. Microstructural analysis of the classic snowball garnets of southeast Vermont: Evidence for non-rotation. Journal of Metamorphic Geology: 10, 567–587.

Hickey, K. A., Bell, T. H. 2001. Resolving complexities associated with the timing of macroscopic folds in multiply deformed terrains The Spring Hill synform, Vermont. Bulletin of the Geological Society of America: 113, 1282–1298.

Ishii, K., Sawaguchi, T. 2002. Lattice- and shape-preferred orientation of orthopyroxene porphyroclasts in peridotites: an application of two-dimensional numerical modelling. Journal of Structural Geology: 24, 517–530.

Kündig, R. 1989. Domal structures and high-grade metamorphism in the Higher Himalayan Crystalline, Zanskar region, northwest Himalaya, India. Journal of Metamorphic Geology: 7, 43–55.

Law, R. D., Searle, M. P., Simpson, R. L. O. 2004. Strain, deformation slab, Everest Massif, Tibet. Journal of geological Society of London: 161, 305–320.

Lee, J., Hacker, B. R., Dinklage, W. S., Wang, Y., Gans, P., Calvert, A., Wan, J. L., Chen, W. J., Blythe, A. E., McClelland, W. 2000. Evolution of the Kangmar Dome, southern Tibet: Structural, petrologic, and thermochronologic constraints. Tectonics: 19, 872–895.

Lister, G. S., Hobbs, B. E. 1980. The simulation of fabric development during plastic deformation and its application to quartzite: the influence of deformation history. Journal of Structural Geology: 2, 355–370.

Marques, F. O., Coelho, S. 2001. Rotation of rigid elliptical cylinders in viscous simple shear flow: analogue experiments. Journal of Structural Geology: 23, 609–617.

Olesen, N. Ø. 2008. The microfabrics of a porphyroclast-rich quartzitic mylonite, Mjølfjell, Jotun Nappe Complex, Norway. Norwegian Journal of geology: 88, 89–101.

Passchier, C. W. 1987. Stable positions of rigid objects in non-coaxial flow-a study in vorticity analysis. Journal of Structural Geology: 9, 679–690.

Passchier, C. W., Trouw, R. A. J. 1996. Microtectonics. Springer-Verlag, Berlin Heidelberg: 287.

Rolland, Y., Mahéo, G., Guillot, S., Pêcher, A. 2001. Tectono-metamorphic evolution of the Karakorum Metamorphic complex (Dassu-Askole area, NE Pakistan): Exhumation of mid-crustal HT-MP gneisses in a convergent context. Journal of Metamorphic Geology: 19, 717–737.

Sarkarinejad, K., Alizadeh, A. 2009. Dynamic model for the exhumation of the Tutak gneiss dome within a bivergent wedge in the Zagros Thrust System of Iran. Journal of Geodynamics: 30, 1–9.

Sarkarinejad, K., Azizi, A. 2008. Slip partitioning and inclined dextral transpression along the Zagros Thrust System, Iran. Journal of Structural Geology: 30, 116–136.

Stipska, P., Schulmann, K., Hock, V. 2000. Complex metamorphic zonation of the Thaya dome: result of buckling and gravitational collapse of an imbricated nappe sequence, in Cosgrove, J. W., and Ameen, M. S., eds., Forced Folds and Fractures: London. Geological Society Special Publication: 169, 197–211.

Taborda, R., Antunes, J., Marques, F.O. 2004. 2D rotation behavior of a rigid ellipse in confined viscous simple shear: numerical experiments using FEM. Tectonophysics: 379, 127–137.

Vanderhaeghe, O., Teyssier, C., Wysoczanski, R. 1999. Structural and geochronological constraints on the role of partial melting during the formation of the Shuswap metamorphic core complex at the latitude of the Thor-Odin Dome, British Columbia. Canadian Journal of Earth Sciences: 36, 917–943.

Wallis, S. R. 1992. Vorticity analysis in a metachert from the Sanbagawa Belt, SW Japan. Journal of Structural Geology: 14, 271–280.

Wallis, S. R. 1995. Vorticity analysis and recognition of ductile extension in the Sanbagwa Belt, SW Japan. Journal of Structural Geology: 17, 1077–1093.

Whitney, D. L., Teyssier, C., Vanderhaeghe, O. 2004. Gneiss domes and crustal flow.

Geological Society of America, Special Paper 380.

Yan, D. -P., Zhou, M. -F., Song, H., Fu, Z. 2003.Structural style and tectonic significance of the Jianglang Dome in the eastern margin of the Tibetan Plateau, China. Journal of Structural Geology: 25, 765–779.